Molecular Vision 2017; 23:1081-1092 <http://www.molvis.org/molvis/v23/1081>
Received 18 June 2017 | Accepted 30 December 2017 | Published 31 December 2017

Upregulation of multiple signaling pathways by Dock5 deletion in epithelial cells

Xiaohe Xu,[1] Hisayoshi Yoshizaki,[1,2] Yasuhito Ishigaki,[3] Eri Kubo,[4] Hiroshi Minato,[5] Etsuko Kiyokawa[1]

(The first two authors contributed equally to this work.)

[1]Department of Oncologic Pathology, Kanazawa Medical University, Ishikawa, Japan; [2]Department of Pediatric Surgery, Kanazawa Medical University, Ishikawa, Japan; [3]Division of Molecular and Cell Biology, Research Institute, Kanazawa Medical University, Ishikawa, Japan; [4]Department of Ophthalmology, Kanazawa Medical University, Ishikawa, Japan; [5]Department of Diagnostic Pathology, Ishikawa Prefectural Central Hospital, Ishikawa, Japan

Purpose: Rupture of lens cataract (RLC) is a hereditary mouse model that shows spontaneous rupture of the lens at the posterior pole at 45–100 days of age. The responsible gene for this phenotype was identified as *Dock5*, a guanine nucleotide exchange factor for small GTPase Rac1. This study was performed to elucidate the pathway initiating this phenotype.
Methods: We examined the RNA expression by microarray in lens epithelial cells (LECs) from wild-type and RLC mice at the pre-rupture age of 21 days. We applied the list of altered genes to an Ingenuity Pathway Analysis (IPA) to predict the pathways that are altered upon dedicator of cytokinesis-5 (Dock5) protein loss. The activation status of the predicted pathways was examined by western blotting in the cultured epithelial cells treated with a Dock5 inhibitor.
Results: The highest-scored network was "Antimicrobial Response, Inflammatory Response, Dermatological Diseases and Conditions." In that network, it is predicted that extracellular signal-regulated kinase (Erk) is activated in LECs from RLC mice. Our test confirmed that Erk was more phosphorylated in the LECs at the equator in both Dock5-knockout mice and RLC mice. In an in vitro experiment of the cultured epithelial cells, the inhibition of Dock5 activity significantly induced Erk activation. It was also confirmed that Akt (cellular homolog of murine thymoma virus akt8 oncogene, also called protein kinase B) and nuclear factor-kappa B (NFκB), predicted to be the key molecules in two other high-scoring networks by IPA, were activated upon Dock5 inhibition in the cultured epithelial cells.
Conclusions: Dock5 participates in epithelial cell maintenance by regulating gene expression.

The rupture of lens cataract (RLC) mouse shows a spontaneous rupture of the lens capsule at the posterior pole, followed by dislocation of the inner nucleus, at 45–100 days of age [1]. RLC is inherited as a single autosomal recessive gene mapped to the middle of mouse chromosome 14 [2]. Fine mapping of the mutant locus has revealed a nucleotide deletion of 27 bp at the end of the 15th exon of *Dock5*, a member of the Dock gene superfamily [3]. We showed previously that the dedicator of cytokinesis-5 (Dock5) protein was hardly detectable in RLC mice, although *Dock5* mRNA was expressed [3]. This finding indicated that Dock5 protein loss is responsible for the rupture of the lens capsule. However, the mechanisms underlying this phenomenon have not been identified.

Dock180 was originally identified as one of two major binding proteins of the adaptor protein CT10-regulated kinase (Crk) [4]. Genetic and biochemical studies later revealed that Dock180 functions as a guanine-nucleotide exchange factor (GEF) for a small GTPase, Rac1 [5]. Orthologs of Dock180 in *Caenorhabditis elegans* and *Drosophila melanogaster* have been identified as cell death abnormal 5 (Ced-5) and myoblast city (Mbc), respectively, and together with Dock180, they comprise an evolutionarily conserved protein group called the CDM (CED-5, Dock180, MBC) family [6]. In addition, studies in *C. elegans* have identified orthologs of Crk (Ced-2) and Rac (Ced-10), showing that the Crk-Dock180-Rac signaling pathway is evolutionally conserved [7].

Dock180's responsible domain for Rac1 activation has been mapped to Dock homology region 2 (DHR-2) [8]. According to the amino acid sequences of their DHR-2 domain, the 11 Dock family members can be divided into four subgroups, namely Dock-A to D [8]. Dock180, Dock5, and Dock2 belong to the Dock-A subfamily, and it has been confirmed that they activate Rac1 [3,5,9]. Interestingly, they are expressed differently in various tissues. For example, Dock180 is expressed in tissues other than peripheral blood leukocytes (PBLs) [4,5] and gene targeting of Dock180 has revealed its essential role in embryonic development [10].

Dock2 rather than Dock180 is expressed in PBLs, as well as in the spleen and thymus [9]. The expression of Dock5 in

Correspondence to: Etsuko Kiyokawa, Kanazawa Medical University Oncologic Pathology 1-1, Daigaku, Uchinada, Kahoku-gun, Ishikawa 920-0293 Japan; Phone: 81-76-286-8116; FAX: 81-76-286-6926; email: kiyokawa@kanazawa-med.ac.jp

osteoclasts [11], neutrophils [12], mast cells [13], and skeletal muscles [10] has been confirmed. Dock2 is expressed in mouse neutrophils and mast cells, and Dock180 is expressed in mouse skeletal muscles; thus, only the depletion of the Dock5 protein shows a modest phenotype [10]. We previously observed that Dock180 is not expressed in the mouse eye, although Dock5 is [3]. Thus, it has been concluded that, among the Dock-A subfamily members, Dock5 is the only functional protein in the mouse eye, and loss of its expression has been shown to result in the degeneration of lens epithelial cells (LECs) and fibers in RLC mice [1,3].

The initial histological changes in the lenses of RLC mice are irregular swelling, condensation, degeneration, and fragmentation of the lens fibers in the deep cortex at 35 days of age [1]. The Dock5 protein is mainly expressed in the LECs, but it is also weakly present in the fiber cells [3]. Therefore, we hypothesized that the loss of Dock5 in the LECs changes the expression of the proteins to affect the morphology of the lens fiber cells. To test this hypothesis, we examined the mRNA expression from the LECs of RLC mice at an earlier age of 21 days, to extract the signaling pathways activated upon Dock5 depletion.

METHODS

Mice: The RLC mutation was first found in a male mouse from the CXSN/A strain [1], a recombinant inbred strain between BALB/cHeA and STS/A mice. The mutant was crossed once with a BALB/cHeA female and maintained by sister-brother mating over 20 generations to establish the mutant line RLC/Stm, which is homozygous for the mutant gene *rlc*. BALB/c mice were used as the wild-type (WT) control unless otherwise noted. The Dock5-knockout (KO) mouse, which is generated by disrupting the Dock5 locus by the retroviral insertion of a β-geo cassette in the intron flanked by exons 29 and 30, was a gift from Dr. Jean-Francoise Cote [10]. Genomic DNA from tail or finger biopsies was extracted using Genomic DNA extraction kits (Lyppo; Gene Modification R&D, Osaka, Japan), and the mouse genotypes were determined by PCR analyses, as described previously [3,10]. The animal protocols were reviewed and approved by the Animal Care and Use Committee of Kanazawa Medical University.

Total RNA preparation, reverse transcription, and quantitative PCR: After CO_2 anesthesia and dislocation of the neck, the mouse eyes were extracted. For LEC isolation, the eyes were soaked for several minutes in PBS (Nissui, Tokyo, Japan), and the layers of the basement membrane and LECs were stripped from the lens nucleus cores under a stereomicroscope. The LECs were prepared from 21-day-old RLC and WT mice. The total RNA was prepared from the pooled LECs from 5 to 8 mice for each experiment using an RNA purification kit (RNeasy Mini Kit; Qiagen, Valencia, CA), as described previously [14,15]. First, 500 ng of total RNA was reverse-transcribed with reverse transcriptase (ReverTraAce; Toyobo, Osaka, Japan) in 20 µl of reaction mixture. Real-time PCR was performed with a SyBr Green PCR system (SYBR® Green Realtime PCR Master Mix; Toyobo). Real-time PCR primers were designed using Primer3Plus as follows: C-type lectin domain containing 11A (*CLEC11A*; F: 5′-ACT GGG GTG GGA AAT GAG G-3′; R: 5′-AGG GTT GGG ACT AGA AGA AGG TG-3′), ubiquitin specific peptidase 18 (*USP18*; F: 5′-GAG CAG CAG GAG GAG CAA AC-3′; R: 5′-GGA CGA AAC ATC TCA AGG CAT C-3′), potassium voltage-gated channel subfamily E regulatory subunit 1 (*KCNE1*; F: 5′-GCT TCT TCG GCT TCT TCA CC-3′; R: 5′-AGA CGG CCT TGC CTT TCT C-3′), calpain 6 (*CAPN6*; F: 5′-CAA GGT GGA GAT GAA CCG AAG-3′; R: 5′-ACG GGT GTC GAT ATA AGT GGA AG-3′), fibroblast growth factor 1 (*FGF1*; F: 5′-GGA AAG GCT GGA AGA AAA CCA-3′; R: 5′-GGGAGGGGCAGAAACAAGA-3′), TMPRSS11D (forward: 5′-CGG CTT TGG TTT GTT GTG G-3′; R: 5′-ATC CAG TTG CGG TAG GCT GT-3′), and glyceraldehyde 3-phosphate dehydrogenase (*GAPDH*; F: 5′-AAT GAA GGG GTC GTT GAT GG-3′; R: 5′-AAA ATG GTG AAG GTC GGT GTG-3′).

The mRNA levels were normalized by the GAPDH mRNA level. Real-time PCR data were quantified using an Excel Macro designed for Gene Expression Analysis with an iCycler iQ real-time PCR detection system, which was provided by Bio-Rad (Hercules, CA).

Microarray analysis: For the Affymetrix microarray, labeled cRNAs were synthesized from sample RNA using a MessageAmp II-Biotin Enhanced Kit (Ambion, Carlsbad, CA). Target hybridizations were performed on a CanGene-1_0-st GeneChip (Affymetrix, High Wycombe, UK) according to the manufacturer's protocol. The hybridized cRNAs were washed and stained in a GeneChip Fluidics Station 450, and signals were detected using a GeneChip Scanner 3000 (Affymetrix). Digitalized image data were processed using the GeneChip Operating Software (GCOS). Fold increases in the signal intensities of the selected genes were calculated using the GeneSpring GX software (Agilent Technologies, Santa Clara, CA). The RNA extraction and microarray analysis were independently performed twice.

Ingenuity Pathway Analysis: The dataset contained gene identifiers and corresponding expression values. It was uploaded into the Ingenuity Pathway Analysis (IPA) software

(Ingenuity Systems, in the public domain), as described previously [16].

Immunohistochemistry: After CO_2 anesthesia and dislocation of the neck, the mouse eyes were extracted. For the immunostaining of activated extracellular signal-regulated kinase (Erk), paraffin-embedded eye sections were prepared and incubated with the antibody against phospho-142 Erk1/2 (pErk) Thr202/Tyr204 (Cell Signaling Technology, Beverly, MA). The bound antibody was visualized by SimpleStain Mouse MAX PO (Nichirei Biosciences, Tokyo, Japan) according to the manufacturer's protocol.

Quantification of pErk in the lens: The LEC in the monolayer at the equator was designated as cell #1, and the next cell toward the anterior pole was designated as cell #2. The number of cells with or without positive staining in the nucleus, cytoplasm, or both was counted until 10 negative cells appeared. The positivity of the cells was expressed as "positive cells/positive + negative cells" from six equators (i.e., three eyes from three mice). Statistical analysis was performed using GraphPad Prism 5 software (La Jolla, CA).

Cell culture and N-(3,5-dichlorophenyl) benzenesulfonamide treatment: Madin–Darby canine kidney (MDCK) cells were purchased from RIKEN BioResource Center (Ibaraki, Japan, No RCB0995) and validated by the Cell Line Authentication Service (IDEXX BioResearch, Columbia, MO) based on the genetic profile using 14 species-specific single tandem repeat (STR) markers. MDCK cells were maintained in Dulbecco's Modified Eagle Medium (D-MEM, WK0442976, Wako Pure Chemical Industries, Tokyo, Japan) supplemented with 10% fetal bovine serum (FBS; Sigma-Aldrich, St. Louis, MO), 100 units/ml of penicillin, and 100 µg/ml of streptomycin in a 5% CO_2 humidified incubator at 37 °C. Twenty-four hours after seeding to the plastic dish, MDCK cells were treated with or without 100 µM N-(3,5-dichlorophenyl) benzenesulfonamide (C21; Alfa Aesar, Ward Hill, MA) or dimethyl sulfoxide (DMSO) and further cultured for 48 h.

SDS–PAGE and western blotting: Cells were lysed in 1× SDS sample buffer [62.5 mM Tris-HCl (pH 6.8), 12% glycerol, 2% SDS, 0.004% bromophenol blue (BPB), and 10% 2-mercaptoethanol]. After sonication and incubation at 95 °C, the proteins were separated by SDS–PAGE on 10% Supersep precast gels (Wako Pure Chemical Industries), and transferred to polyvinylidene difluoride (PVDF) membranes (Immobilon; Millipore, Bedford, MA). After blocking with Odyssey blocking buffer (LI-COR, Lincoln, NE) for 30 min, the membranes were blotted with various antibodies diluted to 1:1,000 [phospho-Erk1/2, Erk1/2 (Cell Signaling Technology), phospho-nuclear factor-kappa B (NFκB) p65 (Ser536; Cell Signaling Technology), pan Akt (Cell Signaling Technology), and phospho-Akt (Ser473; Cell Signaling Technology)], 1:100 (NFκB p65; Santa Cruz Biotechnology, Santa Cruz, CA), or 1:5,000 (β-tubulin; Sigma-Aldrich) in a solution of Odyssey blocking buffer and Tris-buffered saline, followed by incubation with secondary antibodies. The membranes were then scanned with an Odyssey infrared (IR) scanner. Quantification was performed using Image Studio Lite Software (LI-COR). Statistical analysis was performed using GraphPad Prism 5 software.

RESULTS

Microarray and IPA analysis: To understand the molecular mechanisms induced by Dock5 depletion in the LECs, we performed a microarray analysis for mRNA expression. LECs were isolated from 21-day-old WT mice (BALB/c) and 21-day-old RLC mice, and their RNAs were extracted. The genes that showed at least twofold and 1.5-fold changes in their expression in the RLC compared with the WT mice are listed in Table 1 and Appendix 1 (as an average from two independent experiments). The results from three analyses, that is, GeneSpring GX software, Affymetrix TAC software with analysis of variance (ANOVA), and the mean with standard deviation, are shown (Appendix 1).

To certify the accuracy of the microarray data, we performed a quantitative real time (RT)-PCR analysis of six genes: *CLEC11A*, *USP18*, *KCNE1*, *CAPN6*, *FGF1*, and *TMPRSS11D*. As shown in Appendix 2, the amounts of mRNA detected by RT–PCR showed patterns of increase/decrease that were comparable to those detected by the microarray. The relative expression of these six genes measured by RT–PCR and microarray showed parallel correlations (Appendix 2). Unfortunately, commercially available antibodies against CLEC11A, COL4A6, and CCBE1, which were upregulated in the RLC mice, did not detect the endogenous proteins either in paraffin-embedded eye sections or by western blotting (data not shown).

Using the data of the genes that showed greater up- or downregulation in the RLC mice, we performed an IPA to understand the biological relevance and function of the significantly altered genes (Table 2). IPA is a statistical gene-set-enrichment method in which differentially expressed genes intersect with sets of genes associated with a specific biological function or pathway [17]. The IPA database was manually constructed by trained PhD-level curators based on a review of the literature [17].

As a first step in the IPA, we extracted highly influenced Ingenuity canonical pathways from the genes that showed a >1.5-fold difference between the RLC and WT mice (Appendix 1, "FC1.5_GeneSpring" sheet). Overall, compared

Table 1. The list of up- and downregulated genes in the lens epithelial cells of RLC mice.

Affymetrix id	Symbol	Entrez Gene Name	Fold Change*
10562761	CLEC11A	C-type lectin domain family 11 member A	5.23
10607012	COL4A6	collagen, type IV, alpha 6	4.47
10541307	USP18	ubiquitin specific peptidase 18	4.13
10421697	LACC1	laccase (multicopper oxidoreductase) domain containing 1	3.98
10459496	CCBE1	collagen and calcium binding EGF domains 1	3.22
10462623	IFIT1B	interferon induced protein with tetratricopeptide repeats 1B	2.86
10540085	FBLN2	fibulin 2	2.73
10444780	HLA-B	–	2.73
10366153	RASSF9	Ras association (RalGDS/AF-6) domain family (N-terminal) member 9	2.70
10512315	CCL27	–	2.54
10398075	SERPINA3	serpin peptidase inhibitor, clade A (alpha-1 antiproteinase, antitrypsin), member 3	2.52
10565401	Folh1	folate hydrolase 1	2.29
10393573	LGALS3BP	lectin, galactoside-binding, soluble, 3 binding protein	2.28
10524621	Oasl2	2'-5′ oligoadenylate synthetase-like 2	2.24
10462618	IFIT3	interferon induced protein with tetratricopeptide repeats 3	2.16
10424676	LY6E	lymphocyte antigen 6 complex, locus E	2.04
10345101	COL9A1	collagen, type IX, alpha 1	2.01
10562576	PLEKHF1	pleckstrin homology and FYVE domain containing 1	−2.01
10510399	MASP2	mannan-binding lectin serine peptidase 2	−2.04
10440989	KCNE1	–	−2.05
10607143	CAPN6	calpain 6	−2.47
10458560	FGF1	fibroblast growth factor 1 (acidic)	−4.75
10530960	TMPRSS11D	transmembrane protease, serine 11D	−5.72

* Average from two independent experiments.

to the WT, 149 genes were differentially expressed in the RLC mice, and among them, 93 and 56 genes were upregulated and downregulated, respectively. Table 2 shows the pathways that were significantly (p<0.05) affected in the RLC mice. In the table, the term “Ratio” denotes the genes changed in the RLC and WT LECs over the predicted genes involved

Table 2. The list of highly influenced ingenuity canonical pathways.

Ingenuity Canonical Pathways	P value	Ratio		Molecules
Role of Pattern Recognition Receptors in Recognition of Bacteria and Viruses	0.0019	5/106	(0.047)	OAS1, IRF7, DDX58, C3AR1, Oas1b
Complement System	0.0024	3/35	(0.086)	MASP2, C1S, C3AR1
Interferon Signaling	0.0027	3/36	(0.083)	OAS1, IRF9, IFIT3
Activation of IRF by Cytosolic Pattern Recognition Receptors	0.0117	3/72	(0.042)	IRF9, IRF7, DDX58
Ethanol Degradation IV	0.0129	2/29	(0.069)	TYRP1, ALDH3A1
Communication between Innate and Adaptive Immune Cells	0.0200	3/109	(0.028)	HLA-B, IL15, B2M
LXR/RXR Activation	0.0204	4/136	(0.029)	PON1, VTN, SCD, TTR
Superpathway of Cholesterol Biosynthesis	0.0257	2/87	(0.023)	IDI1, HSD17B7
Trans, trans-farnesyl Diphosphate Biosynthesis	0.0288	1/10	(0.100)	IDI1
Antigen Presentation Pathway	0.0295	2/40	(0.050)	HLA-B, B2M

in the pathway listed on the left (as "Ingenuity Canonical Pathways"), and the genes involved in the individual pathway are listed on the right (as "Molecules"). We evaluated the significance of the association between the altered genes and canonical pathway using a right-tailed Fisher's exact test to calculate a *p* value determining the probability that the association was explained by chance alone. In this analysis, three of the same genes, that is, *OAS1*, *HLA-B*, and *IRF7*, appeared in different pathways.

Next, an "Ontology analysis" was performed based on the genes' categorization by their functions and related diseases. Figure 1 shows the pathways that were significantly ($p<0.01$) changed in the RLC mice. The graph expresses the -log (*p* value) for each "category of function," revealing that the genes that were altered in the RLC mice showed the greatest enrichment for "Antimicrobial response," "Inflammatory response," and "Dermatological diseases and conditions."

Prediction and confirmation of phosphorylated Erk in Dock5-depleted LECs: To further understand the biological relevance of the differentially expressed genes in the lenses of RLC mice, we used an IPA to explore their relationships and known annotations. The networks that were more affected in the LECs of RLC mice than those of WT mice are listed, and the top 10 biofunction networks affected are listed in Table 3. Notably, gene expression was the most affected network, with a high score of 42, which was for "Antimicrobial Response, Inflammatory Response, Dermatological Diseases and Conditions."

Based on the collected information and data from the literature, the IPA draws a map by connecting the genes changed in RLC mice (Figure 2A). In the present case, this map included nine predicted genes (open objects). Among them, we focused on Erk, which was connected by 10 lines with positive regulation. Erk plays a central role in cell growth [18]. It is a serine/threonine kinase, the activity of which is regulated by phosphorylation [19]. We first examined Erk phosphorylation (pErk) in isolated mouse LECs (mLECs) by western blotting, which revealed that the Erk phosphorylation was below the detectable level (data not shown). Next, we performed immunohistochemistry and observed Erk phosphorylation in the LECs of the WT mice at the equator, but not in the anterior pole (Figure 2B). The higher magnification of the LECs at the equator indicated that the RLC mice showed stronger signals compared with the WT ones (Figure 2C). Moreover, the numbers of positive cells with phosphorylated Erk were higher in the RLC mice compared with the WT mice. During the experiments, we obtained Dock5-KO mice [10] and found that they had a similar eye phenotype to that of the RLC mice at the age of 40–62 weeks (Appendix 3). Similar Erk phosphorylation results were obtained from the Dock5-KO mice (Figure 2D). We quantified the levels of phosphorylated Erk in BALB/c and RLC and C57BL/6 and Dock5-KO mice. As shown in Figure 2E, the number of pErk-positive cells in the RLC lens was significantly higher than that in the BALB/c lens. The level of phosphorylated Erk in the C57BL/6 lens was higher than that in the BALB/c lens. In the Dock5-KO lens, pErk was slightly increased,

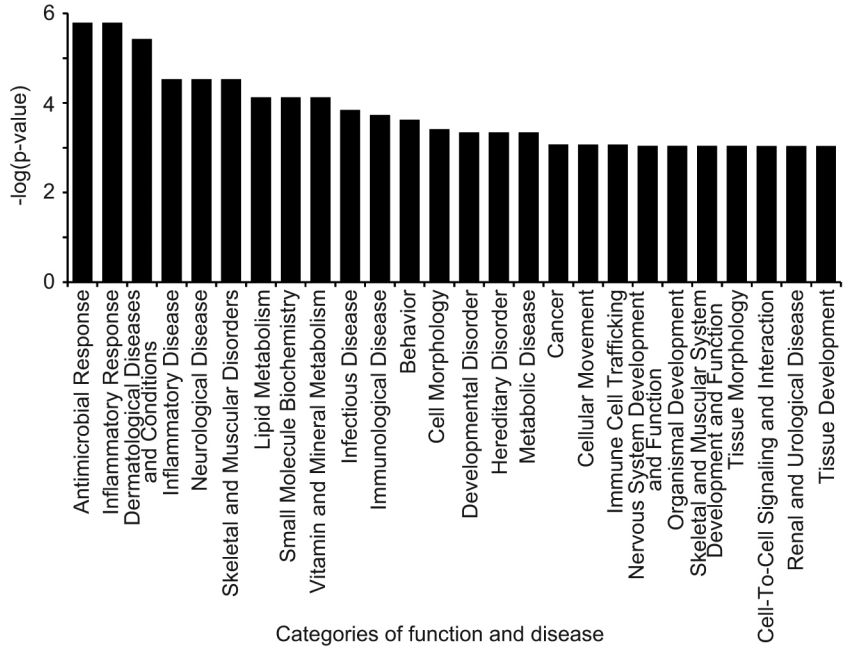

Figure 1. The significantly affected canonical pathways altered in the lens epithelial cells (LECs) upon dedicator of cytokinesis 5 (Dock5) depletion. The canonical pathway analysis was performed using Ingenuity Pathway Analysis (IPA) software. The significant canonical pathways were identified by a p value <0.001.

but not significantly (p = 0.1459). Since we sacrificed the paired mice of BALB/c and RLC, or those of C57BL/6 and Dock5-KO, in one experiment and independently repeated it three times, the average of pErk positivity from each pair of mice was compared. As shown in Figure 2F, in the three BALB/c and RLC pairs, pErk was upregulated in RLC, while in the C57BL/6 and Dock5-KO pairs, pErk upregulation was observed in the two Dock5-KO mice. From these results, we concluded that although phosphorylation of Erk may differ among mouse strains, depletion of Dock5 in LECs induced Erk activation. These results also suggested that, upon Dock5 depletion, the predicted pathway "Antimicrobial Response, Inflammatory Response, Dermatological Diseases and Conditions" is changed to induce Erk activation.

It was previously reported that C21 efficiently inhibits the Rac1 activation induced by Dock5 DHR-2 [11]. To confirm the contribution of Dock5 to Erk activation, we first treated the cultured cell line derived from mLECs with C21 and found that Erk was not activated upon Dock5 inhibition (Appendix 4). The cells exhibited a spindle shape with reduced expression of E-cadherin (Appendix 5), the expression of which is necessary for cell–cell adhesion and the apico-basal polarity of the epithelial cells. Since Rac1 is important for epithelial cell polarity [20], we suspected that altered cell properties, including cell adhesion, polarity, and morphology, may influence gene expression in the mLEC line. We therefore examined the effect of Dock5 inhibition in the MDCK cell line, which has been widely used for epithelial cell research. As shown in Figure 2G, Erk1/2 was phosphorylated in the MDCK cells treated with C21 for 48 h. Quantification confirmed that Dock5 inhibition significantly upregulated Erk phosphorylation (Figure 2H).

To confirm the IPA prediction, we examined two other highly scored networks. In the network with the second highest score, "Lipid Metabolism, Molecular Transport, Small Molecule Biochemistry" (Figure 3A), we found that Akt was predicted to be activated in RLC with eight arrows. Akt (also called protein kinase B), a Pleckstrin homology (PH) domain-containing serine/threonine kinase, has been implicated in the control of diverse cellular functions, including glucose metabolism, gene transcription, cell proliferation, and apoptosis [21]. Upon growth factor stimulation, Akt is phosphorylated at Thr308, then at Ser473, which can be catalyzed by various kinases and can transmit signals to the downstream factors. Therefore, we examined the Ser473 phosphorylation of Akt in MDCK cells treated with C21 for 48 h. As shown in Figure 3B, Akt was phosphorylated in the MDCK by Dock5 inhibition.

Finally, from the map of the third highest network, "Endocrine System Disorders, Gastrointestinal Disease, Metabolic Disease" (Figure 4A), we examined the NFκB activation. NFκB is activated by a wide variety of stimuli. Previously, it was reported that phosphorylation of NFκB p65 (RelA) Ser536 was physiologically induced in response to a variety of proinflammatory stimuli [22]. As shown in Figure 4B, NFκB was significantly phosphorylated in the MDCK by Dock5 inhibition.

DISCUSSION

Our present findings revealed that multiple pathways were affected by Dock5 depletion/inhibition. Based on the predicted networks, we confirmed the activation of three proteins upon Dock5 inhibition in the epithelial cells (Figure 2–4). Since Dock5 possesses no kinase domains,

Table 3. The list of highly influenced networks related diseases and functions by IPA analysis.

ID	Top Diseases and Functions	Score*	Focus Molecules
1	Antimicrobial Response, Inflammatory Response, Dermatological Diseases and Conditions	42	23
2	Lipid Metabolism, Molecular Transport, Small Molecule Biochemistry	39	21
3	Endocrine System Disorders, Gastrointestinal Disease, Metabolic Disease	30	17
4	Lipid Metabolism, Molecular Transport, Small Molecule Biochemistry	27	16
5	Auditory Disease, Auditory and Vestibular System Development and Function, Cell Morphology	25	15
6	Cellular Compromise, Cancer, Cellular Development	24	15
7	Cardiovascular System Development and Function, Organismal Development, Cardiovascular Disease	23	14
8	Cell Death and Survival, Behavior, Cell Cycle	20	13
9	Cellular Development, Cellular Growth and Proliferation, Cellular Movement	11	8
10	Cell-To-Cell Signaling and Interaction, Cell Signaling, Molecular Transport	11	8

* Score indicates the association between the molecules and the networks.

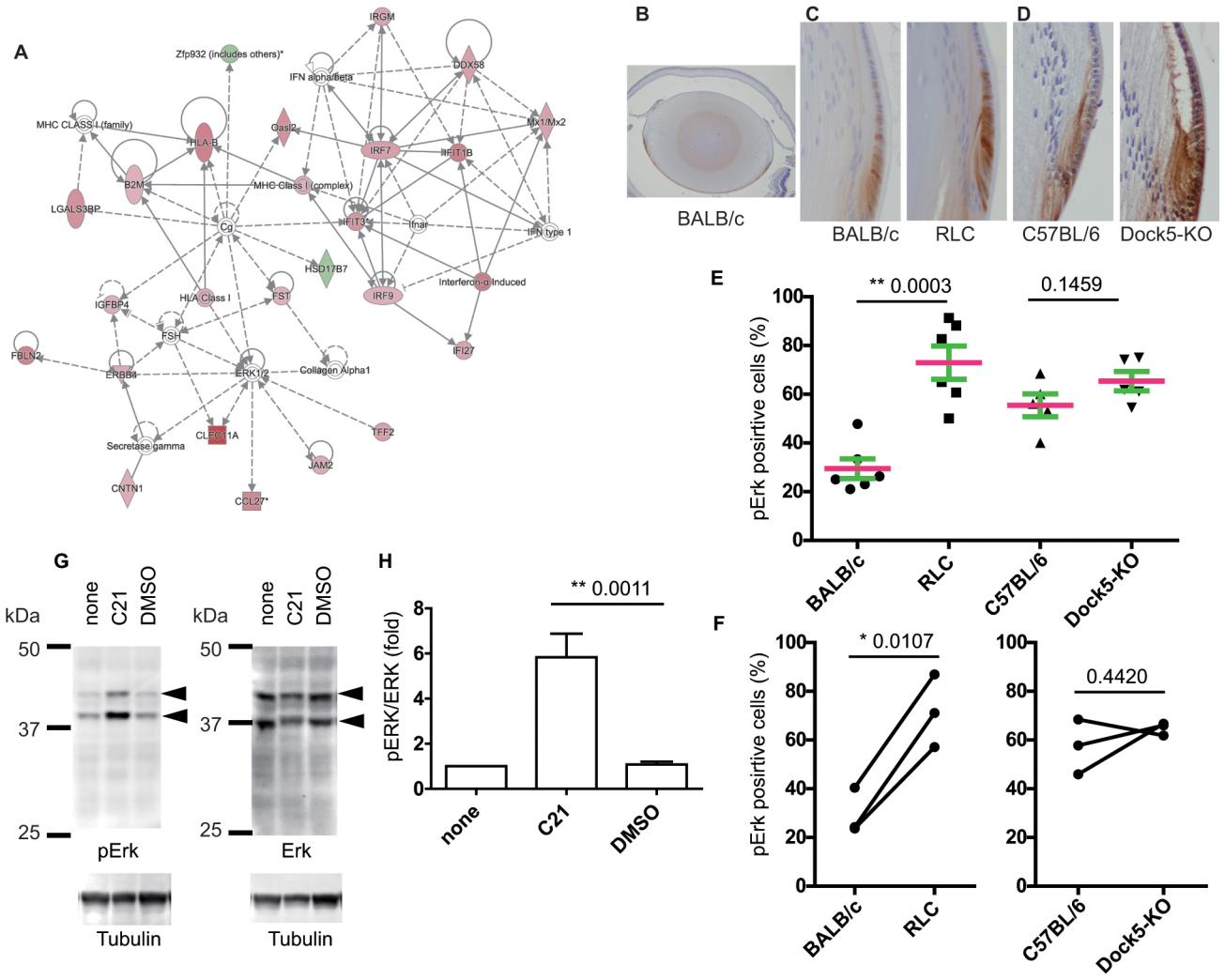

Figure 2. Network analysis and extracellular signal regulating kinase (Erk) phosphorylation upon Dock5 inhibition. **A**: A network analysis of the affected gene expressions in the lens epithelial cells (LECs) of rupture of lens cataract (RLC) mice was performed using Ingenuity Pathway Analysis (IPA) software. In the highest-scored network in the LECs from the RLC mice, "Antimicrobial Response, Inflammatory Response, Dermatological Diseases and Conditions," the protein–protein associations are shown. Nodes are displayed using various shapes that indicate the functional class of the genes: squares, growth factors and cytokines; double circles, group or complex; inverted triangles, kinases; triangles, phosphatases; vertical diamonds, enzymes; horizontal diamonds, peptidases; trapezoids, transporters; vertical ellipses, transmembrane receptors; horizontal ellipses, transcription regulators; and circles, other molecules. The color density of each node indicates the degree of upregulation (red) or downregulation (green) of the respective gene expression. Edges indicate the relationship between the nodes. Arrowheads denote the directionality of the interaction. Perpendicular bars denote an inhibitory interaction. Edges with solid lines indicate a direct interaction, and those with dotted lines indicate an indirect interaction. **B**: The eyes from 21-day-old wild-type (WT; C57BL/6) mice were used for the immunostaining of phosphorylated Erk (pErk). **C**,**D**: Higher magnification of lenses at the equator from a 21-day-old RLC (**C**) and Dock5-knockout (KO) (**D**) mouse and corresponding WT mice (**C**, BALB/c; **D**, C57BL/6). The photographs are representative images from three different mice. **E**,**F**: pErk was quantified as described in the Methods, Results, and Discussion sections. Three mice, that is, six lenses (indicated as black circles, squares, and triangles), were analyzed. In (**E**), the red and green bars denote the average and standard error of the mean (SEM). In (**F**), the pErk positivity is compared in the paired mice. **G**: Madin–Darby canine kidney (MDCK) cells were cultured on a plastic dish and treated with or without N-(3,5-dichlorophenyl) benzenesulfonamide (C21) and dimethyl sulfoxide (DMSO) for 48 h. Cells were washed and subjected to SDS–PAGE and western blotting, with the antibodies indicated at the bottom. **H**: The intensity of the corresponding bands was quantified, and the value of pErk/totak Erk was normalized by the value of the cells without drug treatment (denoted as "none"). The graph shows the averages from six independent experiments with the standard error of the mean (SEM), and the *p* value (0.0011) was calculated using the *t* test. The average ± SEM values were 5.83 ± 1.05 for C21 and 1.08 ± 0.13 for DMSO.

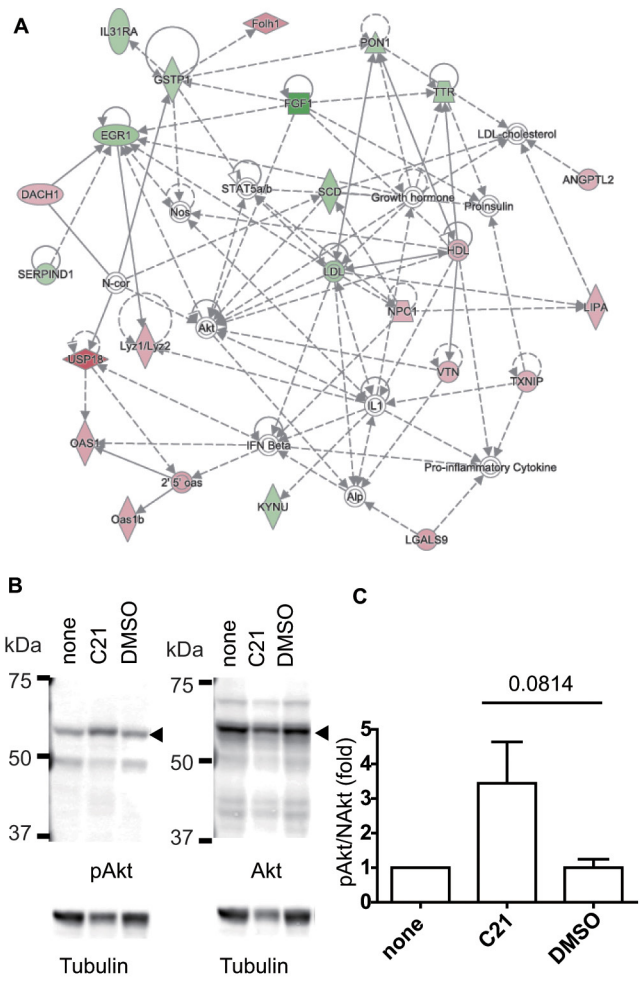

Figure 3. Network analysis and Akt phosphorylation upon Dock5 inhibition. **A**: A network analysis of the affected gene expression in the lens epithelial cells (LECs) of rupture of lens cataract (RLC) mice was performed using Ingenuity Pathway Analysis (IPA) software. In the second highest scored network in the LECs from the RLC mice, "Lipid Metabolism, Molecular Transport, Small Molecule Biochemistry," the protein–protein associations are shown (for details, see Figure 2A). **B**: Madin–Darby canine kidney (MDCK) cells were cultured on a plastic dish and treated with or without N-(3,5-dichlorophenyl) benzenesulfonamide (C21) and dimethyl sulfoxide (DMSO) for 48 h. The cells were washed and subjected to SDS–PAGE and western blotting with the antibodies indicated at the bottom. **C**: The intensity of the corresponding bands was quantified and the value of phosphorylated (cellular homolog of murine thymoma virus akt8 oncogene, also called protein kinase B) Akt/total Akt was normalized by the value of the cells without drug treatment (denoted as "none"). The graph shows the averages from five independent experiments with the standard error of the mean (SEM), and the *p* value (0.0814) was calculated using the *t* test. The average ± SEM values were 3.44 ± 1.20 for C21 and 1.00 ± 0.25 for DMSO.

the upregulation of phosphorylation events is indirect. Our working hypothesis is that the Dock5-Rac1 axis controls various gene expressions, and the inhibition of Dock5-Rac1 in LECs induces changes in gene expression, leading to the activation of multiple signaling cascades and fiber cell degeneration (Figure 5).

Previously, Erk phosphorylation in LECs was observed in the germinative zone and newly differentiating fiber cells of E18.5 WT mice [23]. The present study showed that Erk activation in the lens of adult mice is comparable to that in the embryonic lens, and Dock5 depletion enhances the Erk phosphorylation at the equator. In the experiments using cultured LECs, it was reported that Erk was rapidly activated by transforming growth factor β (TGFβ), which is known to induce the epithelial-mesenchymal transition [24,25]. However, we observed that E-cadherin expression was comparable between LECs from the WT and Dock5-KO or RLC mice (Appendix 6). In addition, the structure of MDCK cells treated with a Dock5 inhibitor remained in the cubital form of the epithelial cells (Appendix 7). Therefore, it was suggested that Dock5 depletion induced Erk activation without an epithelial-mesenchymal transition. Rather, Dock5 depletion induced inflammation responses as predicted by IPA. Since the phosphorylated pattern of Erk was not homogenous in LECs in the adult mice examined here (Figure 2B-D), it is likely that LECs in different locations receive and transmit signals triggered by Dock5 depletion (Figure 5). When the cells express the receptors for the molecules secreted from the epithelial cells, the cells can transmit signals. Since fiber cells and LECs express different proteins, we assume that the signaling events and phenotypes are different between them. Although we could not observe phosphorylation of Erk in

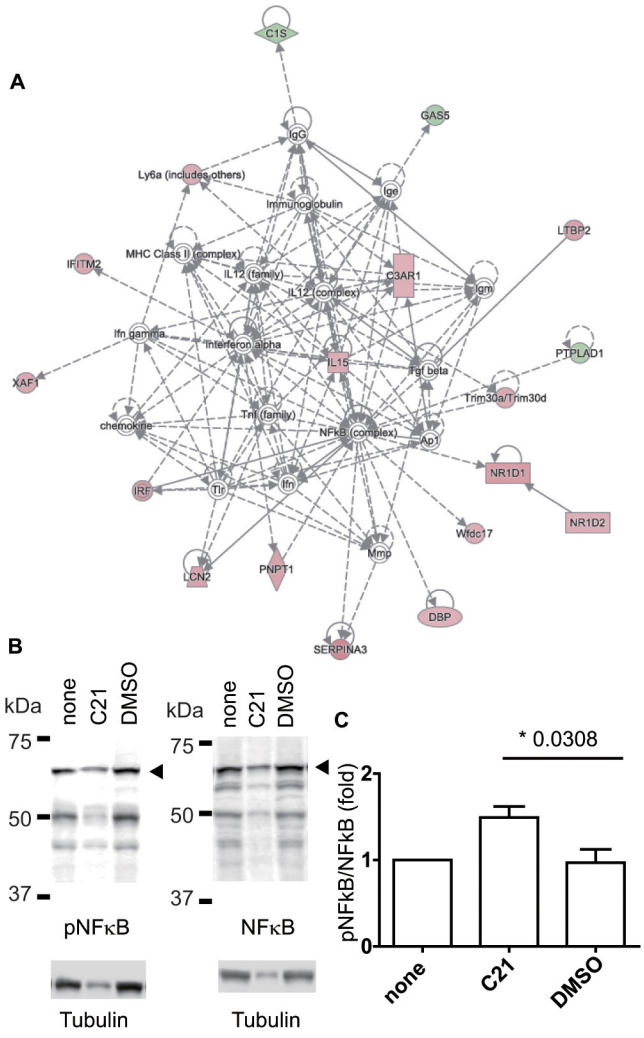

Figure 4. Network analysis and nuclear factor-kappa B (NFκB) phosphorylation upon dedicator of cytokinesis 5 (Dock5) inhibition. **A**: A network analysis of the affected gene expression in the lens epithelial cells (LECs) of rupture of lens cataract (RLC) mice was performed using Ingenuity Pathway Analysis (IPA) software. In the third highest scored network in the LECs from the RLC mice, "Endocrine System Disorders, Gastrointestinal Disease, Metabolic Disease," the protein–protein associations are shown (for details, see Figure 2A). **B**: Madin–Darby canine kidney (MDCK) cells were cultured on the plastic dish and treated with or without N-(3,5-dichlorophenyl) benzenesulfonamide (C21) and dimethyl sulfoxide (DMSO) for 48 h. Cells were washed and subjected to SDS–PAGE and western blotting, with the antibodies indicated at the bottom. **C**: The intensity of the corresponding bands was quantified, and the value of phosphorylated NFκB/total NFκB was normalized by the value of the cells without drug treatment (denoted as "none"). The graph shows the average from five independent experiments with the standard error of the mean (SEM), and the *p* value (0.0308) was calculated using the *t* test. The average ± SEM values were 1.49 ± 0.13 for C21, and 0.97 ± 0.15 for DMSO.

mLECs in this study (Appendix 4), it is possible that Dock5 inhibition induces changes in the gene expression in mLECs that are comparable to those in the mouse lens or MDCK cells, but that mLECs simply lack the receptors to transmit signals.

Several genetically engineered mouse strains exhibit fiber cell degeneration [26,27]. Since most relevant studies have focused on the morphology of the eyes during the development stages, the roles of epithelial and fiber cells in the adults are not fully understood, and the relationship between fiber cell degeneration and lens rupture remains unclear. However, there are reports showing the lens extrusion in the later stages. For example, secreted protein, acidic, and rich in cysteine (SPARC)-deficient mice showed a ruptured capsule at 7 months of age [28]. KO mice of breast cancer anti-estrogen resistance 3 (AND-34/BCAR3), which is associated with $p130^{Cas}$, showed lens vacuolization at postnatal day 3 (P3), followed by lens rupture at P33 [29]. Transgenic (TG) mice of Sprouty, an inhibitory protein against the Erk signaling pathway, showed rupture of the posterior lens capsule by P10 [30]. In the AND-34 KO mice, lower levels of $p130^{Cas}$ expression and Akt phosphorylation were observed in LECs isolated from 4-month-old mice. In Sprouty-TG mice, total Erk1/2 proteins were upregulated, while phosphorylated Erk1/2 was downregulated. Although these phenotypes are comparable to those of RLC and Dock5-KO mice, we were unable to prove that they share the same signaling events. Experiments using Erk or Akt inhibitors must be performed before we can conclude that the inhibition of these proteins in

the epithelial cells of RLC and Dock5-KO mice is required to maintain the ocular morphology.

It is tempting to hypothesize that Dock5 depletion alters the expressions of multiple genes to induce chronic inflammation, which influences LECs and fiber cells in the lens. We found that Akt and NFκB are activated (Figure 3 and Figure 4B), and the second and third predicted networks involve various cytokines (Figure 3 and Figure 4A). In three networks (Figure 2A, Figure 3A, and Figure 4A), no common cytokines or growth factors were listed. Thus, it is plausible that the pathways involving Erk, Akt, and NFκB are triggered by different upstream factors. However, in the previous studies in cultured cells or LEC sheets, hepatocyte growth factor, epidermal growth factor, and fibroblast growth factor activated Erk and Akt simultaneously [30,31,32]. It has been reported that Erk and Akt were both phosphorylated in the lens from phosphatase and tensin homolog (Pten)-KO mice [33]. Because Pten is a negative regulator for Akt, it is plausible that crosstalk exists from Akt to Erk. Since we have now shown that C21 treatment induced Erk, Akt, and NFκB phosphorylation, and there are specific inhibitors against these pathways, further quantitative analysis would be expected to elucidate the detailed signaling pathways for lens maintenance.

APPENDIX 1. THE LIST OF ALTERED GENES IN MICROARRAY ANALYSIS.

To access the data, click or select the words "Appendix 1"

APPENDIX 2. CERTIFICATION OF MRNA EXPRESSION BY RT–PCR.

(A) The relative expression of genes indicated below was quantified by RT–PCR. The values represent the mean of triplicate determinations, and error bars indicate the standard deviation. (B) The values of relative expression of 6 genes detected in the microarray (Microarray, x-axis) in those in RT–PCR (denoted as qPCR, y-axis) were plotted. The approximate line is shown with correlation coefficient (R=0.98). To access the data, click or select the words "Appendix 2"

APPENDIX 3. GROSS EXAMINATION OF CATARACT.

To access the data, click or select the words "Appendix 3"

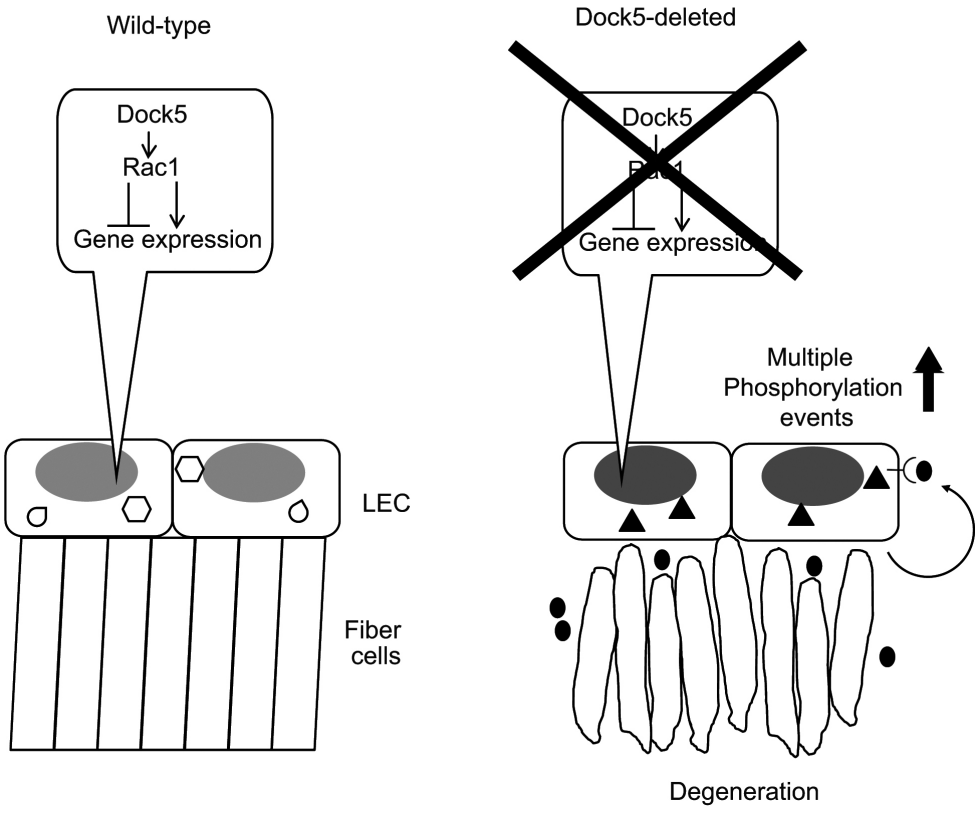

Figure 5. Working model with dedicator of cytokinesis 5 (Dock5) depletion/inhibition.

APPENDIX 4. NO ERK PHOSPHORYLATION IN MLEC TREATED WITH C21.

mLEC cells were cultured on a plastic dish and treated with or without C21 and DMSO for 48 h. Cells were washed and subjected to SDS–PAGE and western blotting with anti-Erk, phosphorylated Erk, and Tubulin antibodies. The intensity of the corresponding bands was quantified and the value of phosphorylated ErK/total ErK was normalized by the value of the cells without drug treatment (denoted as "none"). The graph shows the averages from five independent experiments with the standard error of the mean (SEM), and the *p*-value (0.8951) was calculated using the *t* test. To access the data, click or select the words "Appendix 4"

APPENDIX 5. E-CADHERIN EXPRESSION AND MORPHOLOGY OF MLEC AND MDCK CELLS.

(A) mLEC and MDCK cells were cultured on plastic dishes for several days. After washing with PBS, cells were processed for SDS–PAGE and western blotting as described in METHOD section. Anti-E-Cadherin antibody (cat #3195) was purchased from Cell Signaling. Arrowhead denotes the band corresponding to E-Cadherin. (**B**) and (**C**) mLEC and MDCK cells were cultured on a glass-bottom dish for 48 h, washed with PBS, and fixed with 4% paraformaldehyde. Cells were treated with 0.1% Triton X-100 /PBS for 10 min, and treated with Blocking buffer (Nacalai). Cells were incubated with E-Cadherin antibody, followed by the secondary antibody conjugated with Alexa488 (green), Hoechest 33,342 (blue), and phalloidin-conjugated with Alexa 594. Fluorescent images were obtained with Olympus IX-80. Images in (B) and (C) were obtained with x10 (lower magnification), and x60 lenses, respectively. In mLEC cells, E-Cadherin fluorescent intensity was less compared to MDCK cells, and signals come from the nucleus (B and C). In a negative control (without E-cadherin antibody, but with secondary antibody), such fluorescent signal were not observed. To access the data, click or select the words "Appendix 5"

APPENDIX 6. E-CADHERIN EXPRESSION IN VARIOUS MICE.

IHC was processed as described in METHODS section. Anti-E-Cadherin antibody (cat #3195) was purchased from Cell Signaling. To access the data, click or select the words "Appendix 6"

APPENDIX 7. MORPHOLOGY OF MDCK CELLS TREATED WITH C21.

MDCK cells were treated C21 or DMSO for 48 h and observed with Olympus IX81. To access the data, click or select the words "Appendix 7"

ACKNOWLEDGMENTS

We are grateful to Drs. Hiroshi Hiai and Michiyuki Matsuda (Kyoto University) for the initial preparation of this project, and to Dr. Jean-Francois Cote for providing the Dock5-KO mice. We also thank Y. Inaoka, A. Nakayama, H. Nishihama, Y. Haruta, Y. Kubo, A. Kinebuchi, Y. Nakashima and T. Kanitani for their technical assistance. This work was supported by a Japan Society for the Promotion of Science (JSPS) Kakenhi Grant (no. 25460505).

REFERENCES

1. Iida F, Matsushima Y, Hiai H, Uga S, Honda Y. Rupture of lens cataract: a novel hereditary recessive cataract model in the mouse. Exp Eye Res 1997; 64:107-13. [PMID: 9093026].
2. Matsushima Y, Kamoto T, Iida F, Abujiang P, Honda Y, Hiai H. Mapping of rupture of lens cataract(rlc) on mouse chromosome 14. Genomics 1996; 36:553-4. [PMID: 8884285].
3. Omi N, Kiyokawa E, Matsuda M, Kinoshita K, Yamada S, Matsushima Y, Wang Y, Kawai J, Suzuki M, Hayashizaki Y, Hiai H. Mutation of Dock5, a member of the guanine exchange factor Dock180 superfamily, in the rupture of lens cataract mouse. Exp Eye Res 2008; 86:828-34. [PMID: 18396277].
4. Hasegawa H, Kiyokawa E, Tanaka S, Nagashima K, Gptoh N, Shibuya M, Kurata T, Matsuda M. DOCK180, a major CRK-binding protein, alters cell morphology upon translocation to the cell membrane. Mol Cell Biol 1996; 16:1770-6. [PMID: 8657152].
5. Kiyokawa E, Hashimoto Y, Kobayashi S, Sugimura H, Kurata T, Matsuda M. Activation of Rac1 by a Crk SH3-binding protein, DOCK180. Genes Dev 1998; 12:3331-6. [PMID: 9808620].
6. Wu YC, Horvitz HR. *C. elegans* phagocytosis and cell-migration protein CED-5 is similar to human DOCK180. Nature 1998; 392:501-4. [PMID: 9548255].
7. Reddien PW, Horvitz HR. CED-2/CrkII and CED-10/Rac control phagocytosis and cell migration in *Caenorhabditis elegans*. Nat Cell Biol 2000; 2:131-6. [PMID: 10707082].
8. Côté JF, Vuori K. Identification of an evolutionarily conserved superfamily of DOCK180-related proteins with guanine nucleotide exchange activity. J Cell Sci 2002; 115:4901-13. [PMID: 12432077].
9. Nishihara H, Kobayashi S, Hashimoto Y, Ohba F, Mochizuki N, Kurata T, Nagashima K, Matsuda M. Non-adherent cell-specific expression of DOCK2, a member of the human

CDM-family proteins. Biochimica et Biophysica Acta (BBA) -. Mol Cell Res 1999; 1452:179-87. [PMID: 10559471].

10. Laurin MA, Fradet N, Blangy A, Hall A, Vuori K, Côté JF. The atypical Rac activator Dock180 (Dock1) regulates myoblast fusion in vivo. Proc Natl Acad Sci USA 2008; 105:15446-51. [PMID: 18820033].

11. Vives V, Laurin M, Cres G, Larrousse P, Morichaud Z, Noel D, Côté JF, Blangy A. The Rac1 exchange factor Dock5 is essential for bone resorption by osteoclasts. J Bone Miner Res 2011; 26:1099-110. [PMID: 21542010].

12. Nishikimi A, Kukimoto-Niino M, Yokoyama S, Fukui Y. Immune regulatory functions of DOCK family proteins in health and disease. Exp Cell Res 2013; 319:2343-9. [PMID: 23911989].

13. Ogawa K, Tanaka Y, Uruno T, Duan X, Harada Y, Sanematsu F, Yamamura K, Terasawa M, Nishikimi A, Côté JF, Fukui Y. DOCK5 functions as a key signaling adaptor that links FcγRI signals to microtubule dynamics during mast cell degranulation. J Exp Med 2014; 211:1407-19. [PMID: 24913231].

14. Yoshizaki H, Kuwajima Y, Minato H, Kiyokawa E. Regulation of Ripply1 expression in MDCK organoids. Biochem Biophys Res Commun 2015; 468:337-42. [PMID: 26514726].

15. Yoshizaki H, Ogiso H, Okazaki T, Kiyokawa E. Comparative lipid analysis in the normal and cancerous organoids of MDCK cells. J Biochem 2016; 159:573-84. [PMID: 26783265].

16. Hegde SM, Srivastava K, Tiwary E, Srivastava OP. Molecular mechanism of formation of cortical opacity in CRYAAN101D transgenic mice cortical opacity in CRYAAN101D lenses. Invest Ophthalmol Vis Sci 2014; 55:6398-408. [PMID: 25146988].

17. Kramer A, Green J, Pollard J, Tugendreich S. Causal analysis approaches in Ingenuity Pathway Analysis. Bioinformatics 2014; 30:523-30. [PMID: 24336805].

18. Nishida E, Gotoh Y. The MAP kinase cascade is essential for diverse signal transduction pathways. Trends Biochem Sci 1993; 18:128-31. [PMID: 8388132].

19. Aoki K, Kumagai Y, Sakurai A, Komatsu N, Fujita Y, Shionyu C, Matsuda M. Stochastic ERK activation induced by noise and cell-to-cell propagation regulates cell density-dependent proliferation. Mol Cell 2013; 52:529-40. [PMID: 24140422].

20. Yagi S, Matsuda M, Kiyokawa E. Suppression of Rac1 activity at the apical membrane of MDCK cells is essential for cyst structure maintenance. EMBO Rep 2012; 13:237-243-[PMID: 22261715].

21. Yoshizaki H, Mochizuki N, Gotoh Y, Matsuda M. Akt-PDK1 Complex mediates epidermal growth factor-induced membrane protrusion through Ral activation. Mol Biol Cell 2007; 18:119-28. [PMID: 17079732].

22. Sakurai H, Chiba H, Miyoshi H, Sugita T, Toriumi W. IκB Kinases phosphorylate NFκB p65 subunit on serine 536 in the transactivation domain. J Biol Chem 1999; 274:30353-6. [PMID: 10521409].

23. Xie L, Chen H, Overbeek PA, Reneker LW. Elevated insulin signaling disrupts the growth and differentiation pattern of the mouse lens. Mol Vis 2007; 13:397-407. [PMID: 17417601].

24. Chen X, Ye S, Xiao W, Wang W, Luo L, Liu Y. ERK1/2 pathway mediates epithelial-mesenchymal transition by cross-interacting with TGFbeta/Smad and Jagged/Notch signaling pathways in lens epithelial cells. - Int J Mol Med 2014; 33:1664-70. [PMID: 24714800].

25. Lovicu FJ, McAvoy JW. FGF-induced lens cell proliferation and differentiation is dependent on MAPK (ERK1/2) signalling. Development 2001; 128:5075-84. [PMID: 11748143].

26. Maddala R, Chauhan BK, Walker C, Zheng Y, Robinson ML, Lang RA, Rao PV. Rac1 GTPase-deficient mouse lens exhibits defects in shape, suture formation, fiber cell migration and survival. Dev Biol 2011; 360:30-43. [PMID: 21945075].

27. Maddala R, Nagendran T, Lang RA, Morozov A, Rao PV. Rap1 GTPase is required for mouse lens epithelial maintenance and morphogenesis. Dev Biol 2015; 406:74-91. [PMID: 26212757].

28. Norose K, Clark JI, Syed NA, Basu A, Heber-Katz E, Sage EH, Howe CC. SPARC deficiency leads to early-onset cataractogenesis. Invest Ophthalmol Vis Sci 1998; 39:2674-80. [PMID: 9856777].

29. Near RI, Smith RS, Toselli PA, Freddo TF, Bloom AB, Vanden Borre P, Seldin DC, Lerner A. Loss of AND-34/BCAR3 expression in mice results in rupture of the adult lens. Mol Vis 2009; 15:685-99. [PMID: 19365570].

30. Shin EH, Zhao G, Wang Q, Lovicu FJ. Sprouty gain of function disrupts lens cellular processes and growth by restricting RTK signaling. Dev Biol 2015; 406:129-46. [PMID: 26375880].

31. Tian F, Dong L, Zhou Y, Shao Y, Li W, Zhang H, Wang F. Rapamycin-induced apoptosis in HGF-stimulated lens epithelial cells by AKT/mTOR, ERK and JAK2/STAT3 pathways. Int J Mol Sci 2014; 15:13833-48. [PMID: 25116684].

32. Jiang Q, Zhou CF, Bi ZF, Wan Y. EGF-induced cell migration is mediated by ERK and PI3K/AKT pathways in cultured human lens epithelial cells. J Ocul Pharmacol Ther 2006; 22:93-102. [PMID: 16722795].

33. Chaffee BR, Hoang TV, Leonard MR, Bruney DG, Wagner BD, Dowd JR, Leone G, Ostrowski MC, Robinson ML. FGFR and PTEN signaling interact during lens development to regulate cell survival. Dev Biol 2016; 410:150-63. [PMID: 26764128].

Articles are provided courtesy of Emory University and the Zhongshan Ophthalmic Center, Sun Yat-sen University, P.R. China. The print version of this article was created on 31 December 2017. This reflects all typographical corrections and errata to the article through that date. Details of any changes may be found in the online version of the article.